Applications of coupled mode theory to microcavities with Kerr nonlinearities

Roman Shugayev

April 30, 2014

1 Introduction

Optical frequency comb formation is a very powerful technology, in which optical signals are generated at pre-determined frequency intervals with precisely controlled amplitudes and phases [1]. Optical frequency combs have a number of important current and potential applications, including precision metrology for improved GPS [2, 3], pulse shaping [4], terahertz spectroscopy and sensing, RF modulation [4], quantum photonics [5] and high-harmonic generation for extended UV (XUV) sources for lithography. Typically, optical combs are generated by using a pulsed femtosecond laser. However, such a solution tends to be relatively bulky and expensive. With advances in fabrication techniques, optical frequency combs have been recently fabricated on-chip - a milestone in ultrafast optics, allowing integration and size reduction of the overall system. With a bandwidth of at least an octave (frequencies from ω to 2ω), coherent combs can be interlocked to span a very broad spectrum, enabling the full range of applications mentioned above. However, experimental microresonator combs typically experience too much incoherence for full spectral control at this time. Several theories have been proposed to explain the generation of coherent and incoherent combs, including multilevel comb growth [6] , modulation instability [7], and deterministic chaos [8, 9].

Photonic microresonator frequency combs amenable to on-chip fabrication at small scales have recently attracted significant attention; they enable novel features, including in particular very large (hundreds of GHz or above) free spectral range, increased flexibility in dispersion matching, and especially very high field intensities compared to macroscopic resonators [10, 11]. For four-wave mixing processes, a 1000-fold increase in intensity associated with photonic mode confinement can increase signal and idler generation by a factor of 1,000,000 or more [11].

There have been several theoretical microresonator frequency comb studies performed recently using various approaches such as Lugiato-Lefever (L-L) equation [12, 13] and nonlinear Schrodinger equation [7]. These methods can provide excellent agreement with the experiment [18] on structures that can be approximated as stright waveguides. However they may lead to inaccuracies for small-scale devices such as small radius microresonators and photonic crystals. Additionaly the use of these methods will not be appropriate for multimode-family ananlysis where sub-FSR mode spacing is required. Alternatively, coupled mode theory (CMT) [14–17] circumvents described obstacles and has been extensively used to model nonlinear processes in microcavities. However a one-to-one match between realistic microring comb formation processes and coupled mode theory parameters has not yet been directly demonstrated. In order to study the comb formation in the regime approaching experimental systems we implemented a hybrid CMT / FDTD method. In this approach the key degrees of freedom are modeled through

coupled mode theory with parameters such as mode profiles, mode frequencies and quality factors calculated in finite-difference time-domain (FDTD) simulations.

2 Theory

We can derive the equations of motion for Kerr nonlinear coupled mode theory as follows. We begin with the well-known electromagnetic field Hamiltonian:

$$H = \frac{1}{2}\int dr\ \left[\epsilon E(r)^2 + \frac{1}{\mu}B(r)^2\right] \tag{1}$$

In the presence of a Kerr medium, we can generally write the refractive index as follows:

$$\epsilon(r) = \epsilon_o(r) + \epsilon_2|E(r)|^2 \tag{2}$$

Substituting this expression in yields:

$$H = \frac{1}{2}\int dr\ \left[\epsilon_o(r) + \epsilon_2|E(r)|^2\right]\left[E(r)^2 + \frac{1}{\mu\epsilon}B(r)^2\right] \tag{3}$$

We can assume that we can represent electric field in the single mode k in terms of quadrature operators

$$E_k(r) = C_k \cdot g_k(r)(a_k + a_k^\dagger) \tag{4}$$

where a_k is the annihilation operator, $a_k^\dagger$ is the creation operator and $g_k(r)$ is the normalized amplitude function. C_k is normalization constant.

By normalizing Equation 3 to $\hbar\omega_k$ it can be shown that

$$C_k = \sqrt{\frac{\hbar\omega_k}{2\int \varepsilon_0(r)g_k(r)^2 dr}} \tag{5}$$

By substituting Equation 4 into Equation 1 we can obtain corresponding coupled mode theory equations:

$$H = \sum_k \hbar\omega_k(a_k^\dagger a_k + \frac{1}{2}) + \frac{\hbar^2\varepsilon_2}{8}\sum_{i,j,k,l}\sqrt{\omega_i\omega_j\omega_k\omega_l}M_{ijkl}a_i^\dagger a_j^\dagger a_k a_l e^{i(\omega_k+\omega_l-\omega_i-\omega_j)t} \tag{6}$$

where

$$M_{ijkl} = \frac{\int g_i(r)g_j(r)g_k(r)g_l(r)dr}{\left[\int \varepsilon_0(r)g_i(r)^2dr\right]^{1/2}\left[\int \varepsilon_0(r)g_j(r)^2dr\right]^{1/2}\left[\int \varepsilon_0(r)g_k(r)^2dr\right]^{1/2}\left[\int \varepsilon_0(r)g_l(r)^2dr\right]^{1/2}} \tag{7}$$

3 Numerical Methods

The FDTD simulations in our research are performed using a freely available software package, known as MEEP [19]. To reduce the computational load while preserving accuracy, the system is treated in 2D (which makes the effective height of the ring large). For normal and anomalous dispersion cases we selectively coupled to the modes having fundamental and first harmonic radial profile (order 0 modes and order 1 modes respectively, Fig. 2). The distributed source

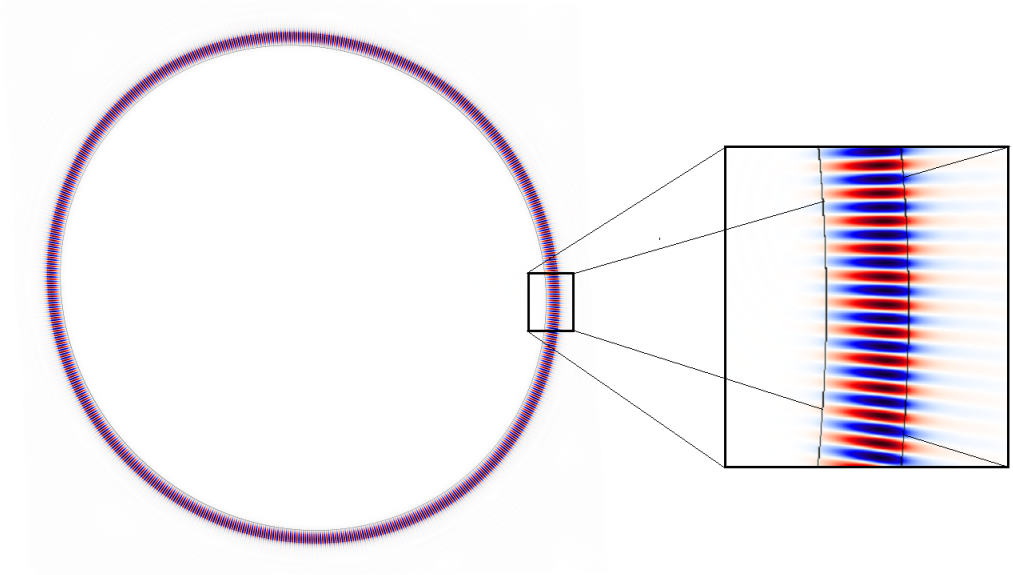

Figure 1: Distribution of the electric field of the mode having fundamental radial profile. Into the plane (E_z) component of the field is shown. Red designates positive values; blue negative; white zero

excitation was positioned within the microring core. It is Gaussian in both time and azimuthal direction such that source amplitude $A_s \propto |A_s| e^{(t-t_0)^2/2\tau^2} e^{(\phi-\phi_0)^2/2\sigma^2}$. In azimuthal direction it is modulated with $e^{ik_\phi \phi}$ where k_ϕ corresponds to the azimuthal wavevector of the "cold" cavity. In the radial direction, for excitation of fundamental mode follows a cos(r) profile with the maximum corresponding to the core center . Similarly for excitation of order 1 mode the radial variation has a sin(r) profile with zero corresponding to the core center. Polarization in all cases is in the z direction (into the plane on figure 1) The source center frequency was chosen to coincide with the natural resonant frequency of the microring computed obtained using filter diagonalization.The values for refractive index were chosen to restrict the number of modes excited in the ring. Geometric dispersion (Fig. 3) was obtained from the frequencies of the resonant modes of the specific family obtained using `harminv`, a filter diagonalization MEEP program.

The CMT frequencies were set to match the linear dispersion slope obtained from `harminv` frequencies.The coupling coefficient M_{ijkl} is computed by assuming perfect spatial mode overlap between modes (following Eq. 7). The resulting system of coupled differential equations is solved using the `ode15s` stiff ODE solver in Matlab.

In order to directly compare FDTD results to CMT simulations, the electrical field E_z in FDTD was sampled at a single point, and compared to a sum of the cavity mode fields in the CMT simulation. The sampling location in FDTD was set at the point inside the microring core corresponding to the maximum of the radial mode profile (Fig. 2).

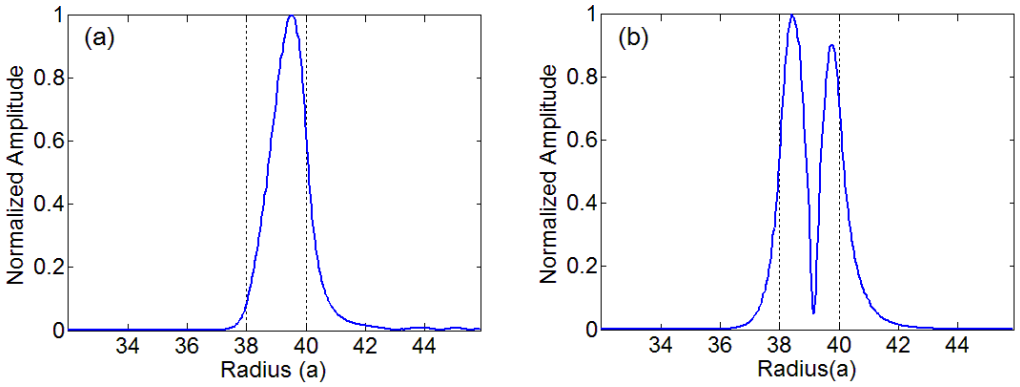

Figure 2: Radial distribution of normalized amplitude function (a) Fundamental normal dispresion mode (b) Order 1 anomalous dispersion mode. Extents of the microring core region are shown in dotted lines.

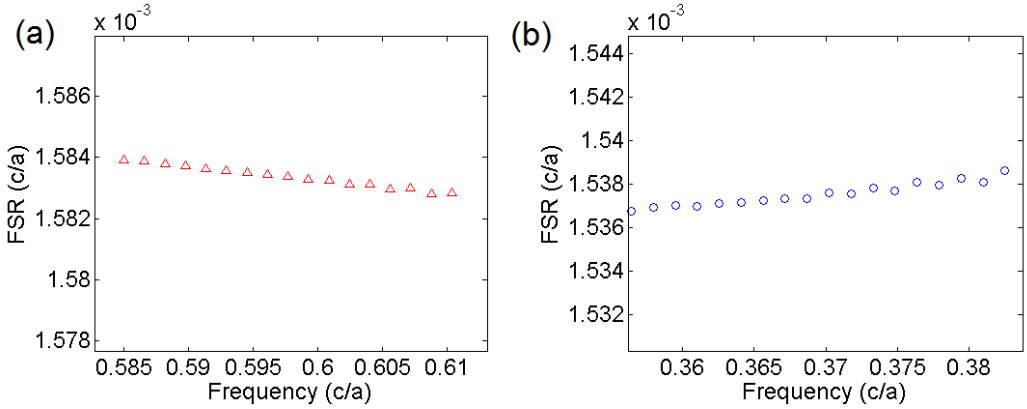

Figure 3: FSR data for normal disperion region of fundamental radial profile modes (a) and anomalous dispersion region of order 1 modes (b)

4 Results

We can show that our expectations of comb generation dynamics are confirmed with direct finite-difference time domain simulation, and show the corresponding coupled-mode theory simulations that corroborate our prior observations.

We can observe a close correlation between FDTD and CMT simulations, both from the time domain (Figs. 4 (a,b), 5 (a,b)) and frequency domain (Figs. 4 (c,d), 5 (c,d)) perspectives.

In particular the time domain envelopes of CMT and FDTD simulations match very well with key features such as self-phase modulation induced initial peak and beat tones corresponding to round trip times in the cavity. The shapes of the periodic pulses are also closely matched in both cases. The low frequency beat tone present in FDTD anomalous simulation (Fig. 5, (a)) is due to the coupling of the source having a mode 1 profile to the modes of the the other family (mode 0) . This coupling could not be completely eliminated in anomalous case as two modes nearly coincide in frequency and propagation of mode 0 is allowed. In normal case we were able

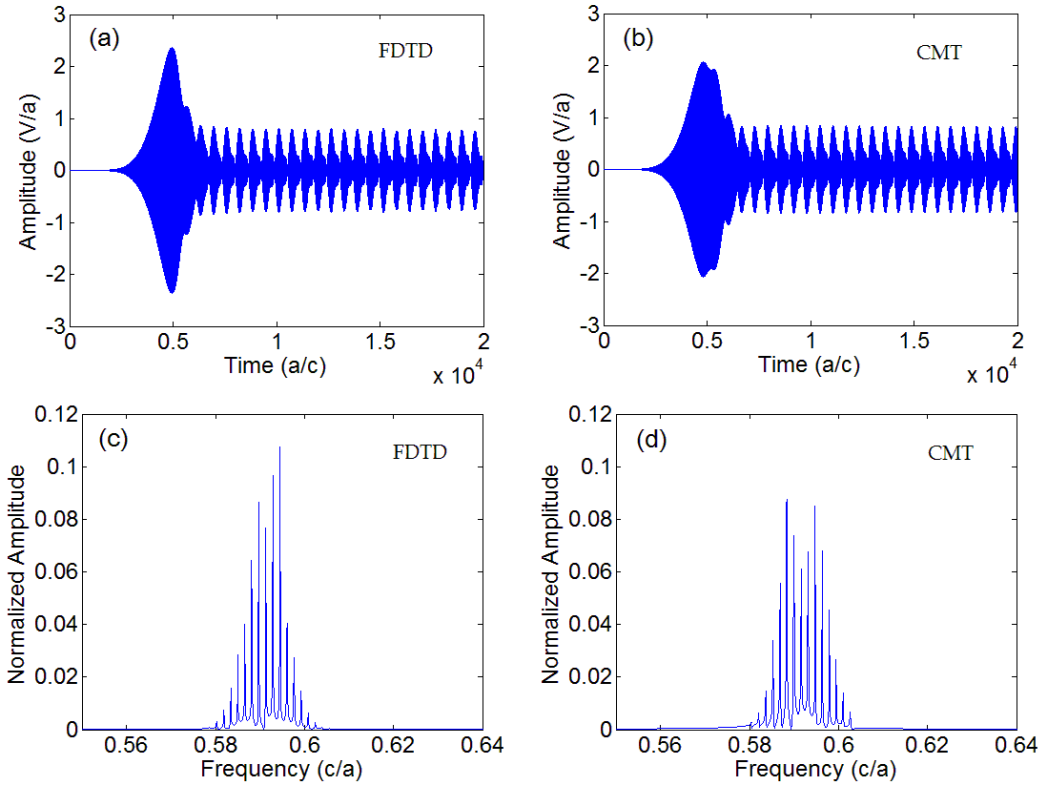

Figure 4: Comparison of FDTD and CMT results for normal disperision case (a) FDTD time domain (b) CMT time domain (c) FDTD frequency domain (d) CMT frequency domain

to prohibit mode 1 propagation by increasing the cladding index hence no low frequency beat tones were observed there.

As far as the frequency domain, the graphs can be seen to match well in terms of their bandwidth and frequency spacing. However, FDTD simulation show a slight asymmetry in its frequency spectrum compared to CMT. We can again observe the effects of undesirable coupling in anomalous case seen as lowering of FDTD spectral amplitude compared to CMT (Fig. 5 (c), (d) as some of the energy is channeled to the modes of the other family.

We further investigated the root cause of the observed asymmetry in the spectrum shape. Taking advantage of the CMT ability to separate different nonlinear coupling mechanisms we perform the time domain envelope comparison of FDTD with CMT selectively disabling different CMT coupling channels (Fig. 6, (a)) . We compare simulations done using full CMT approach, CMT with only self-phase modulation (SPM) terms included and CMT with both SPM and cross-phase modulation (XPM) terms included. The case of CMT simulation with only SPM terms gives us a very good match with initial FDTD transient while FDTD with both SPM and XPM terms quenches the initial peak. This implies that magnitude of XPM interactions in FDTD is reduced from those in CMT during the initial phase. To explain this we can further note that onset of CMT XPM interactions occurs as the envelope of the source starts to flatten-Gaussian input waveform reaches its peak. Indeed when Gaussian reaches its maximum value (Fig. 6, (a) black arrow) the amplitudes of the sideband modes are stabilized and coupling

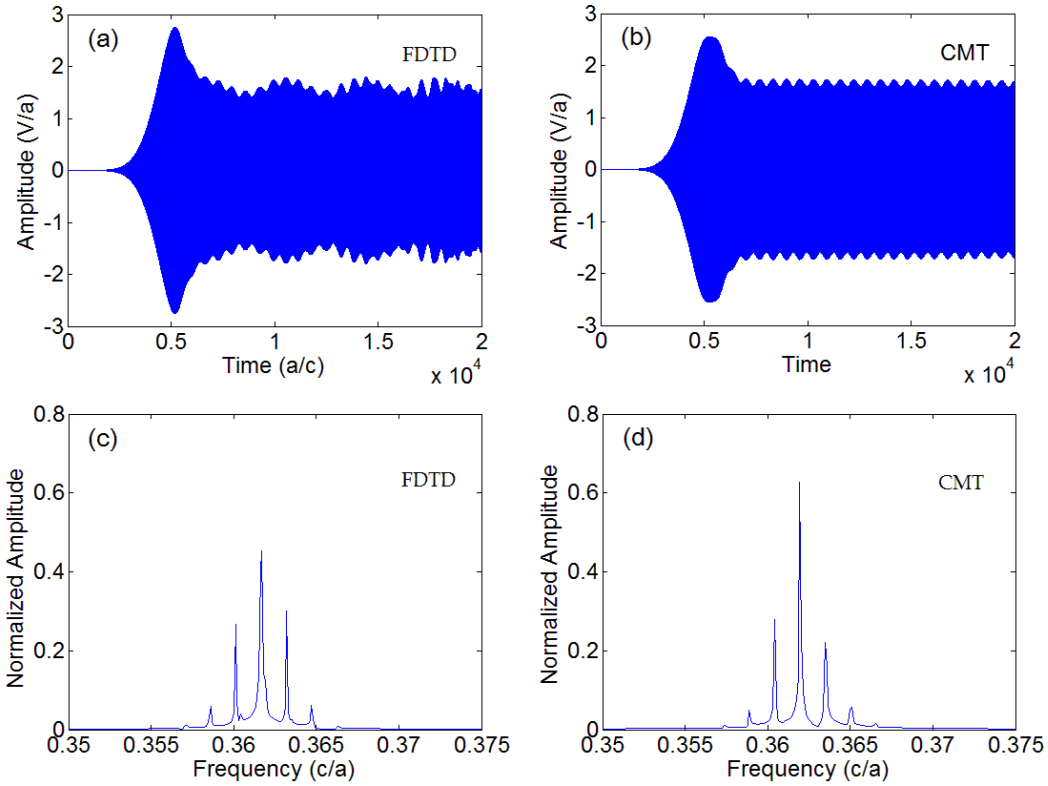

Figure 5: Comparison of FDTD and CMT results for anomalousl disperision case (a) FDTD time domain (b) CMT time domain (c) FDTD frequency domain (d) CMT frequency domain

with the pump mode will occur. However in FDTD microring system this stabilization does not take place everywhere simultaneously but rather being reached gradually as the pulse propagates around the cavity. Therefore the onset of the full XPM coupling will be delayed and overall XPM coupling magnitude during the initial phase will be reduced. In other words, initial conditions on the pulse formation will not be perfectly matched to the FDTD with the current CMT source. However, it seams feasible to design a more complex source that will emulate the effects described above if one was to achieve a better accuracy in the frequency domain envelope.

As an alternative, a natural course of action would be to attempt to use an FDTD source with a spatially uniform envelope . Figure 6, (b) shows the results for sources with uniform distribution and source with angular standard deviation $\sigma = 3.14$ rad. Same as before the amplitudes we set to produce 5 V/a uniform "cold " cavity mode amplitude; the source bandwidth and nonlinear coefficient were held the same. Our results suggest that having a uniform source does not produce enough intermode coupling to generate a comb from a single pump line, and that nonuniform "seeding", similar to modulation instability onset is required. In theory spontaneous emergence of the modes with the uniform source can be achieved by properly setting the noise floor but we anticipate that in that case obtained spectrum would be even more difficult to predict. This assumption will have to be verified by future research.

In all cases, the simulation times can be dramatically reduced by going from FDTD to CMT simulations. It took approximately 5 hours with 48 cores to run the FDTD simulation in MEEP

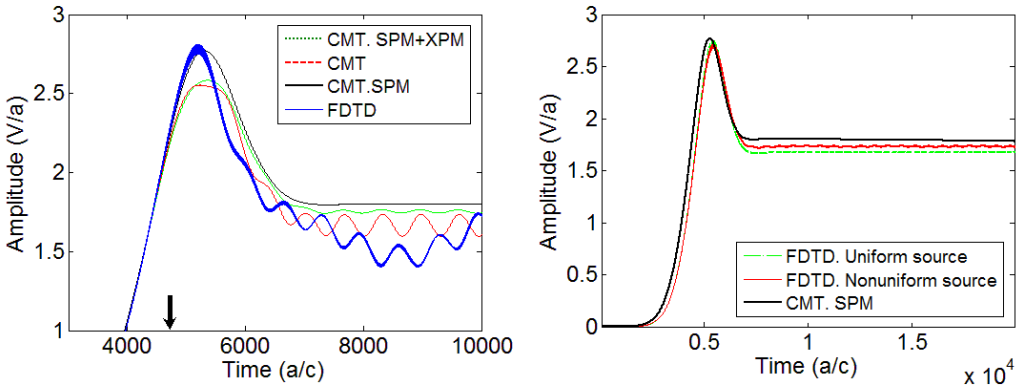

Figure 6: Timed domain envelopes of different coupling and excitation regimes in FDTD and CMT. (a) Comparison of FDTD and CMT envelopes for different coupling mechanisms (blue solid) FDTD results, (dashed red) CMT results, (black solid) CMT results with only self-phase modulation (SPM) terms, (dotted green) CMT results with only SPM and cross-phase modulation (XPM) terms. Black arrow indicates peak time of Gaussian source. (b) Comparison of FDTD and CMT for different excitation regimes (dotted green) uniform source, (solid red) source with $\sigma = 3.14$, (solid black) CMT results with only SPM terms

on the Purdue University Rosen Center for Advanced Computing's Carter Community Cluster. Note that the simulation was performed on 2D system with the infinite third dimension. For the full 3D system the simulations time would be further multiplied. In the 2D case MEEP scales well for this problem up to 48 cores and beyond – i.e., the number of core-hours consumed is not strongly dependent on the number of cores used. However, the CMT simulation with our current Matlab implementation only took 20 minutes as a serial process (single-core) on an Asus desktop machine. This represents a decrease in CPU core-hours by a factor of 720, or equivalently, 2.86 orders of magnitude. These results thus demonstrate a clear advantage in using the CMT method versus a fully vectorial approach. In future work, it would be desirable to achieve an even greater degree of improvement through fine-tuning of the ODE solution technique embedded in MATLAB. Subsequent topics for investigation may then include detailed exploration and optimization of microresonator comb design as a function of experimental parameter values, assuming modest nonlinear coefficients. A search technique such as this could enable a broad range of customized applications for these combs, which may include but would not be limited to: signal and idler pair generation at arbitrary, targeted frequencies; enhanced third-harmonic generation; efficient terahertz generation; and arbitrary waveform generation.

Overall we demonstrated the approach that can help to simplify analysis of coupled modes interaction in presence of nonlinear medium, while providing additional insight to complex dynamics of this process . It was shown that the results of the direct FDTD and CMT simulations match each other fairly closely. The exceptions to perfect matching are due to cross-coupling of FDTD excitation and imperfect initial condition matching. The approach can be used to examine the generation of optical combs in the presence of dispersion (both normal and anomalous), and our studies showed that comb generation from the single pump line is still permitted in both cases. Furthermore, the number of CPU core-hours required for the CMT simulation is reduced by a factor of 720 compared to the FDTD simulation, and may be amenable to further reductions. This substantial speed-up should enable comprehensive automated design and optimization studies to achieve microresonator combs with tailored properties. The new com-

putational framework can be leveraged for analyzing important optical applications of nonlinear phenomena in photonic crystals, plasmonics and metamaterials. The approach can be readily transfered to the analysis of weakly coupled system having nontrivial mode distribution and coupling such as random lasers, laser focusing on nanoscale, high harmonic generation, pulse shaping and quantum photonics.

References

[1] P. Del'Haye, A. Schliesser, O. Arcizet, T. Wilken, R. Holzwarth, and T. J. Kippenberg, "Optical frequency comb generation from a monolithic microresonator," Nature **450,** 1214 (2007).

[2] J. Ye and S.T. Cundiff,*Femtosecond Optical Frequency Comb: Principle, Operation, and Applications* (Kluwer, Norwell, MA, 2005)

[3] P. Del'Haye, S.B. Papp, S.A. Diddams," Hybrid Electro-Optically Modulated Microcombs" , Phys. Rev. Lett. **109,** 263901 (2012)

[4] I. S. Grudinin, N. Yu, and L. Maleki, "Generation of optical frequency combs with a CaF_2 resonator," Opt. Lett. **34**, 878-880 (2009).

[5] W. C Jiang, X. Lu, J. Zhang, O. Painter, Q. Lin, "A silicon-chip source ofbright photon-pair comb," Preprint at http://arxiv.org/abs/1210.4455v1 (2012).

[6] T. Herr , K. Hartinger, J. Riemensberger,, C.Y. Wang, E. Gavartin, R. Holzwarth, M.L. Gorodetsky, T.J. Kippenberg, Universal formation dynamics and noise of Kerr-frequency combs in microresonators Nature Photon. **6,** 480-7 (2012).

[7] A. B. Matsko, A. A. Savchenkov, W. Liang, V. S. Ilchenko, D. Seidel, and L. Maleki, "Mode-locked Kerr frequency combs," Opt. Lett. **36,** 2845 (2011).

[8] Y.K. Chembo and N. Yu, "Modal expansion approach to optical-frequency-comb generation with monolithic whispering-gallery-mode resonators," Phys Rev. A **82,** 033801 (2010).

[9] E. Granados ,D.W. Coutts, D.J. Spence,"Mode-locked deep ultraviolet Ce:LiCAF laser," Opt. Lett. **34,** 1660-1662 (2009).

[10] M. Popovic, *Theory and design of High-Index-Contrast microphotonic circuits,* MIT libraries thesis collection (2008).

[11] J.D. Joannopoulos, S.G.Johnson, J.N. Winn and R.D. Meade, et al., *Photonic Crystals: Molding the Flow of Light,* Second Edition (Princeton University Press, Princeton, 2007).

[12] L.A. Lugiato, R. Lefever,"Spatial dissipative structures in passive optical systems," Phys. Rev. Lett. **58** 2209 -2211 (1987)

[13] S. Coen, H.G. Randle, T. Sylvestre, M. Erkintalo,"Modeling of octave-spanning Kerr frequency combs using a generalized mean-field Lugiato-Lefever model", Opt. Lett. **38,** 37-39 (2013)

[14] A. Yariv, P. Yeh *Photonics: optical electronics in modern communications,* Oxford University Press (2007)

[15] A. B. Matsko, W. Liang, A. A. Savchenkov, L. Maleki "Chaotic dynamics of frequency combs generated with continuously pumped nonlinear microresonators", Opt. Lett. **38,**, 525-527 (2013)

[16] T. Hansson, D. Modotto, S. Wabnitz "On the numerical simulation of Kerr frequency combs using coupled mode equations" Opt. Comm., **312,** 134 (2014)

[17] M. Peccianti, A. Pasquazi, Y. Park, B.E. Little, S.T. Chu, D.J. Moss and R. Morandotti "Demonstration of a stable ultrafast laser based on a nonlinear microcavity" Nature Comm.,**3,** 765 (2012)

[18] M.R. Lamont, Y. Okawachi,A.L. Gaeta,"Route to stabilized ultrabroadband microresonator-based frequency combs," Opt. Lett. **38** 3478-3481 (2013)

[19] A. F. Oskooi, D. Roundy, M. Ibanescu, P. Bermel, J. D. Joannopoulos, and S. G. Johnson," MEEP A flexible free software package for electromagnetic simulations by the FDTD method, Comp. Phys. Commun. **181,** 687702 (2010).